

Influence of preparation methods on the electrical and nanomechanical properties of poly(methyl methacrylate)/multiwalled carbon nanotubes composites

Katarína Mosnáčková,¹ Zdenko Špitálský,¹ Jaroslav Kuliček,¹ Jan Prokeš,² Amalia Skarmoutsou,³ Costas A. Charitidis,³ Mária Omastová¹

¹Polymer Institute, Slovak Academy of Sciences, Dúbravská cesta 9, 845 41 Bratislava, Slovakia

²Charles University in Prague, Faculty of Mathematics and Physics, Charles University in Prague, 182 00 Prague 8, Czech Republic

³School of Chemical Engineering, National Technical University of Athens, 9 Heroon Polytechniou St., Zographos 157 80, Athens, Greece

Correspondence to: M. Omastová (E-mail: maria.omastova@savba.sk)

ABSTRACT: Poly(methyl methacrylate)/multiwalled carbon nanotubes (PMMA/MWCNT) composites were prepared by two different methods: melt mixing and solution casting. For solution casting, two different solvents, toluene and chloroform, were used to prepare PMMA solutions with different concentrations of MWCNT. The dispersion of the CNT in the composite samples was verified by scanning electron microscopy. For the nanocomposites prepared by both methods, the electrical conductivity increased with increasing filler content, showing typical percolation behavior. In addition, an increase of 11 orders of magnitude in the electrical conductivity relative to the matrix conductivity was determined by broadband dielectric spectroscopy and four probe conductivity measurements. A maximum value of $\sigma_{DC} \sim 1.6$ S/cm was found for the highest filler loaded sample (3.67 vol %), which was prepared by solution casting from toluene. Nanoindentation analysis was used to characterize the surface mechanical properties of the composite samples prepared by the different methods. Indentation tests were performed at various penetration depths, and it was revealed that the melt mixing process resulted in stiffer neat PMMA samples compared to the solution casted PMMA samples. © 2014 Wiley Periodicals, Inc. *J. Appl. Polym. Sci.* **2015**, *132*, 41721.

KEYWORDS: composites; graphene and fullerenes; mechanical properties; nanotubes; synthesis and processing

Received 13 July 2014; accepted 2 November 2014

DOI: 10.1002/app.41721

INTRODUCTION

Since their discovery by Iijima in 1991,¹ carbon nanotubes have been the center of interest of many research efforts due to their unique physical properties, such as large aspect ratio, low mass density, excellent current-carrying capability, high thermal conductivity, and many others. The combination of good mechanical properties and high thermal and electrical conductivity of carbon nanotubes (CNT) make them ideal reinforcing agents for various applications.² A number of thermoplastic polymers, such as poly(methyl methacrylate),³ poly(vinyl chloride),⁴ polypropylene,⁵ polyamide,⁶ and many others, have been used for the preparation of new types of polymer/CNT composites with improved electrical properties. These composites with well-dispersed MWCNT have been produced by several methods, including extrusion techniques,⁷ melt processing,⁸ coagulation methods,⁹ solution processing,¹⁰ and injection moulding.¹¹ Covalent modification can produce strong interfacial adhesion

between the matrix and the fillers, improving the dispersion of the CNT.¹² On the other hand, functionalization partially destroys the π -bonds on the CNT surface, which diminishes the delocalization of electrons and can decrease the electrical conductivity.¹³ These new composite materials can be used as anti-static materials¹⁴ or in flexible electronics,¹⁵ as separation membranes,¹⁶ etc.

Polymer/conducting filler composites are characterized by their percolation behavior compared to traditional materials, where small addition of filler results in significant increase in electrical conductivity. The percolation threshold depends not only on the shape and diameter of the conducting fillers as carbon nanotubes but also on the composite processing and, finally, on the CNT dispersion in the polymeric matrix. A low percolation threshold of ~ 0.12 wt % CNT in a PMMA matrix was achieved by using CNT with high aspect ratios of ~ 1000 , as reported by Chen *et al.*¹⁷ The use of CNT with a ten-fold lower aspect ratio

for preparation of composites caused the increase of percolation threshold to increase to 0.65 wt %.¹⁸ In both cases, the composites were prepared by solution casting and the electrical conductivity at the percolation concentration was on the order of 10^{-3} S/cm. The electrical properties of the composite materials also depended heavily on the preparation conditions, the type of matrix, and their structural characteristics. Du *et al.*⁹ found that the electrical properties are affected by the single walled carbon nanotubes (SWCNT) orientation in the polymeric matrix, and a sample containing 2 wt % CNT produced a significant decrease in electrical conductivity from 10^{-4} to 10^{-10} S/cm after achieving filler alignment. The decrease in conductivity occurred as a result of the reduced conductive contacts in the PMMA matrix after the alignment of the SWCNT.

PMMA/CNT composites are most commonly prepared by melt mixing. Recently, Logakis *et al.*¹⁹ reported a high electrical conductivity of 10^{-2} S/cm at a percolation concentration of 0.75 wt % MWCNT in composites prepared by melt mixing. Khattari *et al.*²⁰ prepared PMMA/MWCNT composites using the same mixing conditions but with a different type of MWCNT. However, their obtained results revealed a percolation threshold ranging between 8.5 and 10 wt % and a lower electrical conductivity of $\sim 2 \times 10^{-8}$ S/cm. McClory *et al.*³ evaluated the influence of the MWCNT particle geometry, the PMMA particle size, and the PMMA/CNT production process on percolation thresholds. Most likely, short arc-discharge manufactured MWCNT are more easily dispersed in the PMMA matrix.³ Pötschke *et al.*⁸ investigated the effects of the melt mixing conditions on the electrical conductivity near the percolation threshold. They found that the screw speed and mixing time strongly influenced the distribution and dispersion of MWCNT at various compositions below and above the percolation threshold. At low MWCNT contents below the percolation threshold, increased screw speeds induced better dispersion, whereas above the percolation threshold, the formation of a nanotube network led to breakage of the MWCNT, resulting in conductivity decreases. In contrast, if mild conditions of melt mixing were used, such as short time and low rate (25 rpm, 15 min), the percolation threshold was achieved at a higher MWCNT loading (18–19 wt %). Insufficient dispersion of the filler at 14.5 wt % MWCNT loading in the polymer matrix was also confirmed by TEM images. If composites were prepared by solution processing involving the dissolution of polymer in solvent and the direct sonication of the polymer solution and the MWCNT, the percolation thresholds was obtained at lower MWCNT loadings.²¹ The best result was achieved for samples prepared from toluene with percolation at 4 wt %. Additionally, higher percolation thresholds of ~ 7 wt % and 10 wt % were observed for composites prepared from chloroform and acetone, respectively.²¹

In this study, we report the preparation of PMMA/MWCNT composites by melt-mixing and solution processing using chloroform and toluene as solvents. Non-functionalized multiwalled carbon nanotubes were used as filler. A systematic study of the effects of various processing methods on the electrical conductivities of PMMA/CNT composites has not previously been reported. The aim of this work was to find the optimal processing method for the preparation of composite materials with both

the lowest percolation concentration and good filler dispersion. We focused on the electrical properties of PMMA/MWCNT using the direct current mode (σ_{DC}) measured by two or four-point probe measurements and the alternative current mode (σ_{AC}) using broadband dielectric spectroscopy (BDS). The electrical percolation threshold (p_c), which represents the critical composition of conducting inclusions, was calculated from the obtained data. Furthermore, the nanomechanical properties of the PMMA/CNT composites were evaluated via nanoindentation testing. Through nanoindentation, it was possible to investigate the mechanical behavior of the composites at low applied loads and correlate their resistance with their electrical conductivity and preparation process. In addition, the morphologies of the prepared composite materials, which can influence their conductivity, were investigated by SEM.

EXPERIMENTAL

Materials

PMMA Plexiglas® 7N (density 1.19 g/cm³), in pellet form from Röhm GmbH. (Germany), was used as the polymeric matrix. Multiwalled carbon nanotubes (MWCNT), Nanocyl™ 7000 (density 1.66 g/cm³), were delivered from Nanocyl S.A. (Sambreville, Belgium). MWCNT were produced by chemical vapour deposition (CVD) with an average diameter of 9.5 nm, an average length of 1.5 μ m, and a carbon purity >90%.²² Chloroform, toluene, acetone, and *N,N*-dimethylformamide were supplied from AFT Bratislava (Slovakia) with a purity >99%.

Nanocomposite Preparation by Melt Mixing

All components specified for mixing were dried in an oven under vacuum. The PMMA pellets were dried for 2–3 h at 80°C, MWCNT for 2 h at 120°C, respectively. The nanocomposites were mixed in a micro-compounder with a 15 mL chamber (DSM Xplore, The Netherlands) at 230°C at a mixing speed of 100 rpm for 10 min. The extruded strands were cut for pressing into the form of sheets using a hydraulic press (Fontijne SRA-100, The Netherlands) at 200°C and 10 bar for 3 min.

Nanocomposite Preparation by Solution Casting

Appropriate quantities of MWCNT were dispersed in solvent (100 mL) by sonication using the ultrasonic processor UP400S (Hielscher, Germany) with sonotrode H7 (diameter 7 mm) in 100% pulse mode with an acoustic power density of 320 W/cm² and a frequency of 24 kHz for 20 min. Solutions of PMMA in chloroform and toluene at a concentration of 0.1 g/cm³ were mixed by a magnetic stirrer at 50 °C. When the PMMA pellets were completely dissolved, a dispersion of MWCNT varying from 0 to 3.67 vol % in concentration (corresponding 0–5.0 wt %) was added. Stirring was carried out for 1 h, whereupon the prepared composite was poured on a Teflon foil. After evaporation of the solvent, the composites were dried in a vacuum oven with a gradually increasing temperature from 35°C to 80°C for few hours. The samples were pressed in the same way as described above for the melt mixed composites.

Experimental Techniques

The DC electrical conductivities of the compressed pellets with a diameter of 13 mm and a thickness of 1 mm were determined

by a four-point van der Pauw method using a Keithley 237 High-Voltage Source Measurement Unit (Keithley) and a Keithley 2010 Multimeter (Keithley) equipped with a 2000-SCAN 10 Channel Scanner Card. When the conductivity of the sample was below 10^{-4} S/cm, a two-point method using a Keithley 6517 electrometer (Keithley) was used. Before such measurements, circular gold electrodes were deposited on both sides of the pellets. Usually 4–5 samples from each composite were measured, and the mean value was recorded.

Broadband dielectric spectroscopy (BDS) measurements were performed by a Novocontrol Concept 40 with an Alpha dielectric spectrometer provided by Novocontrol Technologies GmbH (Hundsangen, Germany). The BDS-1200 parallel-plate capacitor with two gold-plated electrodes was used as a test cell and was supplied by Novocontrol Technologies. The diameter of the specimens was 10 mm, and the thickness was ~ 0.2 mm. The DC and AC parameters were measured after vacuum depositing gold electrodes (10 mm in diameter) on both sides of the pelletized samples to ensure electrical contact. The AC properties were measured using precision LCR meters HP4284A and HP4285A in the frequency range of 0.001 Hz –40 MHz at room temperature.

The indentation tests were performed using a Hysitron Ubi1® nanomechanical test instrument (Hysitron). The instrument was equipped with a transducer with the ability to exert loads in the range of 1–10,000 μ N with a high load resolution of 1 nN, while the maximum penetration depth that could be recorded was 3000 nm (3 μ m) with a resolution of 0.04 nm. A three-sided pyramidal Berkovich diamond indenter (100 nm tip radius) was used to measure the stiffness (S), hardness (H), and reduced modulus (E_r) values. On the basis of the half-space elastic deformation theory, H and E_r values can be extracted from the obtained unloading curves using the Oliver and Pharr method,^{23,24} whereas the derived expressions for calculating the elastic modulus from indentation experiments are based on Sneddon's elastic contact theory.²⁵ The instrument was also equipped with a Scanning Probe Microscope (SPM), in which the probe tip was moved in a raster scan pattern across the sample surface using a three-axis piezo positioner.

Scanning electron microscopy (SEM) measurements were performed using a ZEISS EVO 40HV (Germany) electron microscope. The composite microstructures were investigated at a cryo-fractured surface in liquid nitrogen after sputtering with gold.

RESULTS AND DISCUSSION

Melt mixing techniques and solution casting are currently the most suitable methods for the preparation of CNT composites with a low percolation threshold and good electrical conductivity. For PMMA/CNT composites prepared by solution casting methods, different conditions of ultrasonic treatment have been reported. Krause *et al.*²⁶ investigated the dispersion of MWCNT in different solvents after a short ultrasonic treatment for 3 min. The best dispersion of MWCNT (Nanocyl™ NC 7000) was achieved in chloroform, where homogenous black dispersions appeared. On the other hand, swollen agglomerates of

MWCNT were found in acetone, n-hexane, and petroleum ether. Slobodian *et al.*²¹ used the same solvents for the preparation of PMMA/MWCNT composites, but ultrasound treatment was carried out in the presence of polymer matrix for 10 min. The best result was achieved using toluene, where the percolation threshold was found at a 4 wt % MWCNT loading. In this study, the dispersion of MWCNT in four solvents, that is, chloroform, toluene, acetone, and *N,N*-dimethylformamide, was investigated. Only in chloroform and toluene did the Nanocyl™ NC7000 MWCNT create a stable dispersion after sonication (using a power density of 320 W/cm² for 20 min under cooling in an ice bath). On the basis of these tests, these two solvents were selected as the best solvents for the preparation of the composites.

Morphological Characterization

SEM was used to evaluate the CNT dispersion in the matrix and to study the morphology of the neat PMMA matrix prepared by solution casting in chloroform and toluene, as shown in Figure 1(a,b). In the next step, the morphologies of the composites below and above the percolation threshold were studied (see part Electrical properties). As observed from the SEM micrographs (Figure 1), the composites prepared by solution casting from both solvents using 0.55 vol % [Figure 1(c,d)] and 1.44 vol % MWCNT [Figure 1(e,f)] showed good dispersion without any agglomeration. At the cryo-fractured cross section, MWCNT ~ 1 μ m in length were visible at higher magnifications (not shown here). The results of SEM analysis indicated that the solution method is a suitable and non-destructive technique for composites preparation. We concluded that the conditions of preparation were suitable. Longer mixing times and ultrasound treatments led to the breakage of the original MWCNT agglomerates. Figure 2 presents SEM images of the PMMA matrix and PMMA/MWCNT composites prepared by melt mixing with 0.55 and 1.44 vol % MWCNT. In the melt mixed composite containing 0.55 vol % MWCNT a smaller amount of filler compared to the solution cast samples was detected in the cross section [Figure 2(b)]. Unlike the composites prepared by the solution method, for the composites prepared by melt mixing, short MWCNT were observed. Generally, it is assumed that CNT can be shortened during melt mixing. Despite the flexible structure of CNT, compared with carbon fibers, prolonged mixing time can result in conductivity decrease.⁸ Thus, the shorter MWCNT observed in the SEM images can be attributed to CNT shortening due to the high shear forces during melt mixing, which resulted in lower conductivities compared to the samples prepared by solution casting (see subsequent discussion). On the other hand, only the protruding parts of the MWCNT from the brittle fracture of composites were observed. In both MWCNT loadings (0.55 and 1.44 vol %), a homogenous distribution of filler in the sample cross sections with no aggregation was observed.

Electrical Properties

The DC electrical conductivities of composites with MWCNT concentrations varying from 0.36 to 3.67 vol % were investigated using four and two probe measurements (Figure 3). For the composites prepared by melt mixing, the percolation threshold was above a 0.6 vol % MWCNT loading. For the

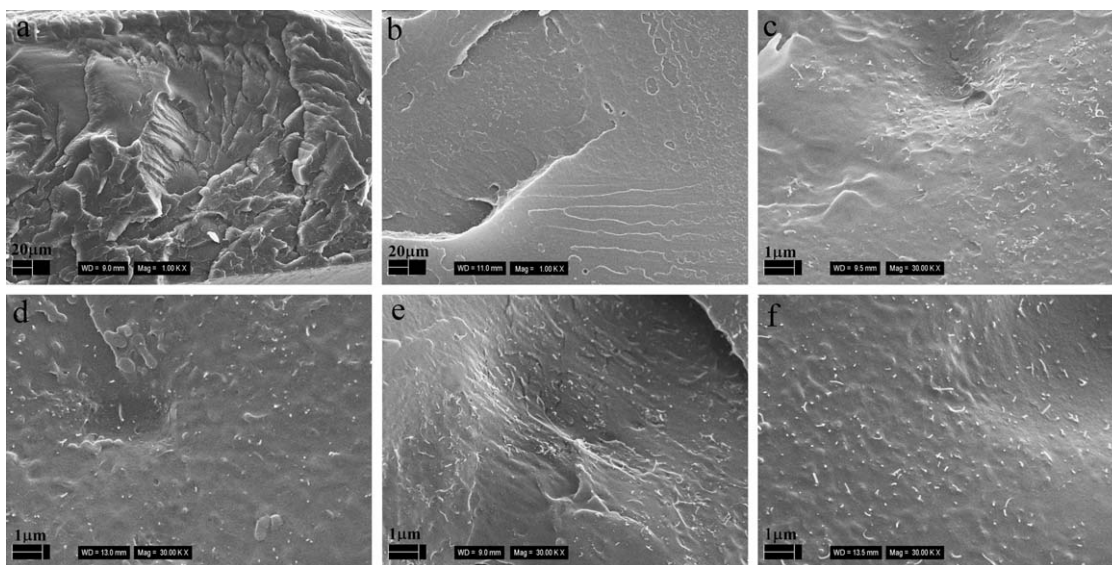


Figure 1. SEM images of neat PMMA casted from chloroform (a), and toluene (b), and of PMMA/MWCNT composites containing 0.55 vol % MWCNT (c and d), and 1.44 vol % MWCNT (e and f) prepared by solution casting in (c and e) chloroform, and (d and f) toluene.

composites prepared by solution casting, the electrical conductivity σ_{DC} increased significantly after the addition of just 0.36 vol % of filler. The electrical conductivity σ_{DC} of PMMA after the evaporation of both solvents was $\sim 1.70 \times 10^{-16}$ S/cm. After the addition of 0.36 vol % MWCNT σ_{DC} increased ~ 14 orders of magnitude to 3.39×10^{-2} S/cm and ~ 12 orders of magnitude to 1.63×10^{-4} S/cm for the composites prepared from chloroform and toluene solutions, respectively. This sharp increase in the electrical conductivity of solution cast composites indicated that the percolation threshold was achieved at a lower concentration of CNT, i.e., $p_c < 0.36$ vol % (corresponding to 0.5 wt %). The composites prepared by melt mixing also achieved lower conductivity values at higher nanofiller loadings, which can be attributed to the diminished dispersion of the CNT. Dielectric measurements using alternating current were employed to composites prepared by solution casting, in order to precisely determine the percolation thresholds.

Figure 4(a–c) presents the real part of the electrical conductivity σ' as a function of the frequency of the PMMA matrix and the MWCNT loading in the composite, which included 0.36, 0.55, 0.75, 1.10, 1.44, 2.17, 2.90, and 3.67 vol % at room temperature. PMMA is an insulating material and has a typical dielectric response corresponding to a linear increase in σ'

with increasing frequency. In the case of the melt mixed composites [Figure 4(a)], this dielectric behavior was also observed for samples prepared with 0.36 vol % CNT because the many isolated nanotubes acted as nanocapacitors. The electrical conductivity of the composite with a 0.36 vol % MWCNT loading was close to that of neat PMMA (2.66×10^{-14} S/cm). This can most likely be attributed to the inadequate dispersion of the MWCNT in the polymer matrix by melt mixing. For higher concentrations of MWCNT (0.55 vol %), the dependence of the real part of the electrical conductivity on the frequency displayed two different behaviors [Figure 4(a)]. In the lower frequency range, the conductivity σ' did not change with increasing frequency due to the gradual formation of a nanotubes network, and its value corresponded to the conductivity measured by direct current methods (σ_{DC}). Distinct regions imply the existence of different dissipating effects and are characteristic of semiconductors. At the lower frequencies, < 10 kHz, the conductivity is found to increase with increasing frequency, describing the electrodes polarization phenomena, and is followed by the frequency independent plateau region at higher frequencies.²⁷ In the high frequency region, the relationship between the real part of the conductivity σ' and the frequency follows the universal dielectric response law:

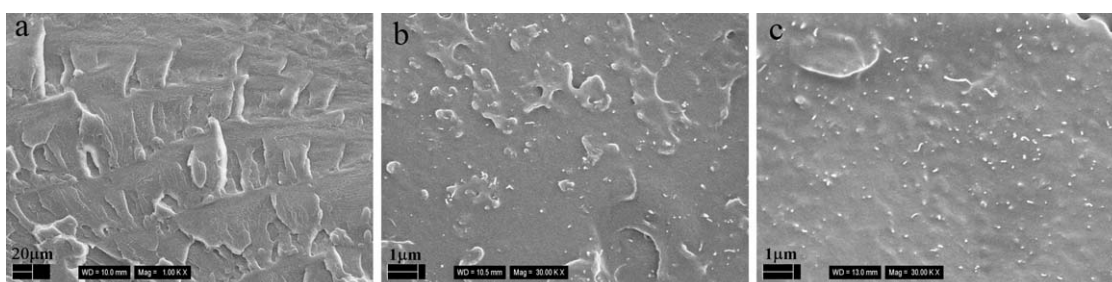


Figure 2. SEM micrograph of neat PMMA matrix (a), and PMMA/MWCNT composites prepared by melt mixing and containing 0.55 vol % (b), and 1.44 vol % (c) MWCNT.

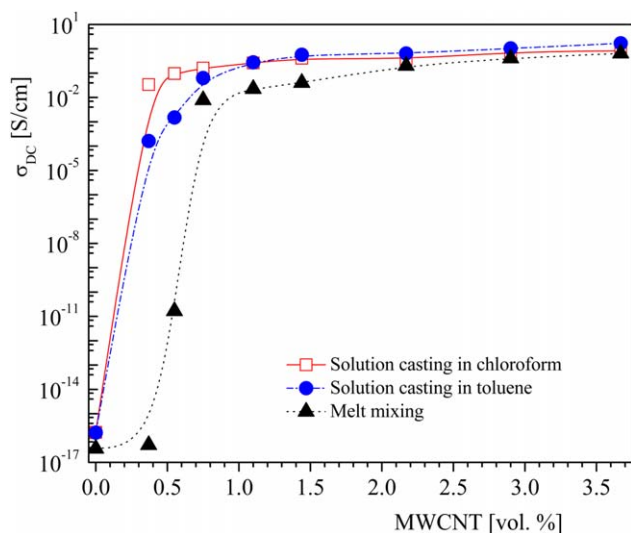


Figure 3. The dependence of σ_{DC} on the amount MWCNT for composites prepared by melt mixing and solution casting measured at room temperature. [Color figure can be viewed in the online issue, which is available at wileyonlinelibrary.com.]

$$\sigma = Af^n \quad (1)$$

where f is the frequency, A is the dielectric constant that depends on the electrode polarization, and n is a constant close to 0.6.²⁸

However, above the percolation concentration, the electrical conductivity increased with MWCNT loading and was independent on frequency in the measured range at room temperature. For the nanocomposites prepared by solution casting, an almost 10 orders of magnitude higher conductivity compared with the neat PMMA matrix was observed at a 0.36 vol % MWCNT loading [Figure 4(b,c)]. Moreover, the conductivity was independent on the frequency. These results indicated that the percolation threshold for nanocomposites prepared by solution casting is lower than 0.36 vol % of MWCNT. For this reason additional composite samples were prepared by solution casting from chloroform, containing 0.07, 0.22, and 0.29 vol % of CNT (corresponding to 0.1, 0.3, and 0.4 wt %). As it is presented in Figure 4(b), composites containing already 0.07 vol % of filler are conductive reaching value 10^{-4} S/cm.

The percolation thresholds were precisely calculated by linear fitting with respect to the scaling law²⁹ for the experimental data in Figure 5:

$$\sigma_{DC} \approx (p - p_c)^t \quad (2)$$

where σ_{DC} is the DC conductivity, p_c is the percolation threshold, p is the volume fraction of the filler, and t is the exponent characterizing the dimensionality of the investigated conductive system.

For the composites prepared by melt mixing, the best fit for the percolation threshold was obtained at a volume fraction of 0.49 ± 0.08 and a critical exponent t of $\sim 2.84 \pm 0.14$. Logakis *et al.*¹⁹ reported for the same composite a p_c of 0.75 wt % MWCNT (0.55 vol %), which corresponds very well with the p_c value obtained by our calculations. The composite containing 3.67 vol % (5 wt %) CNT achieved an AC conductivity of

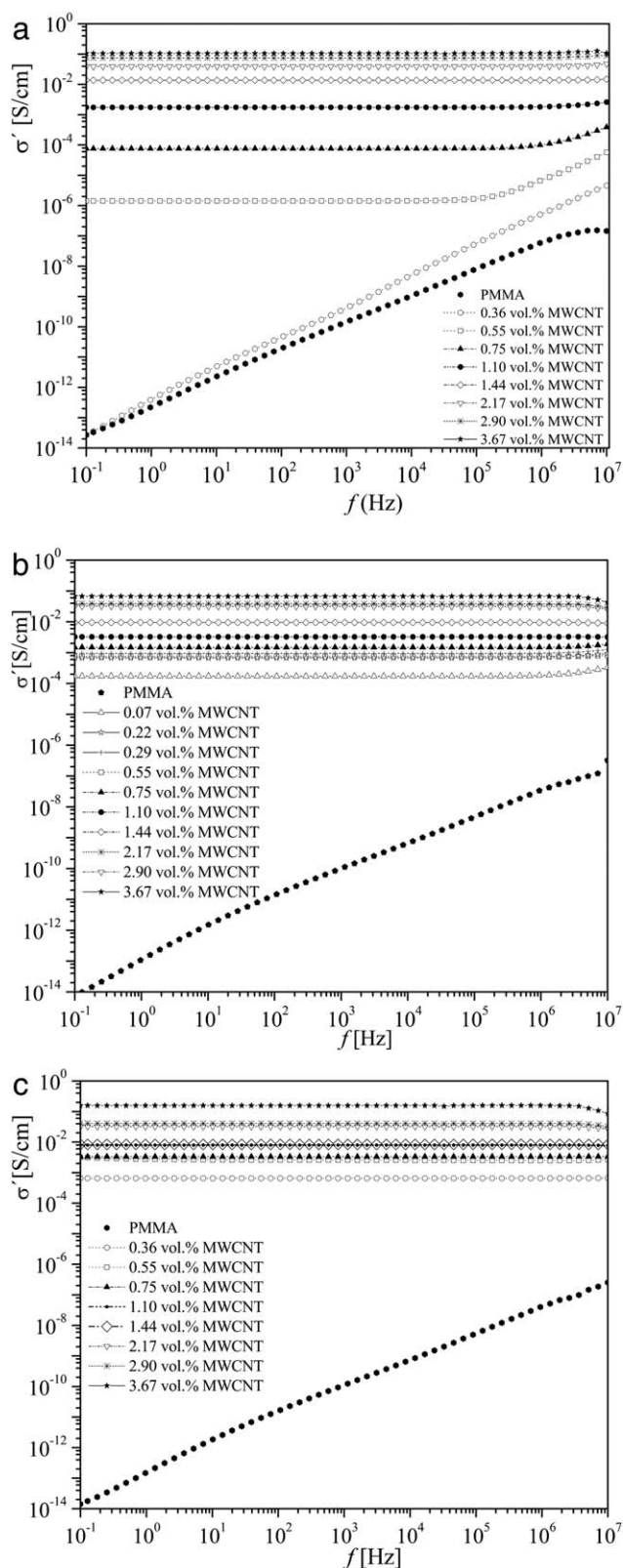


Figure 4. The real part of the electrical conductivity σ' as a function of frequency for all composites prepared by melt mixing (a), and solution casting in toluene (b), and in chloroform (c) with various amounts of MWCNT.

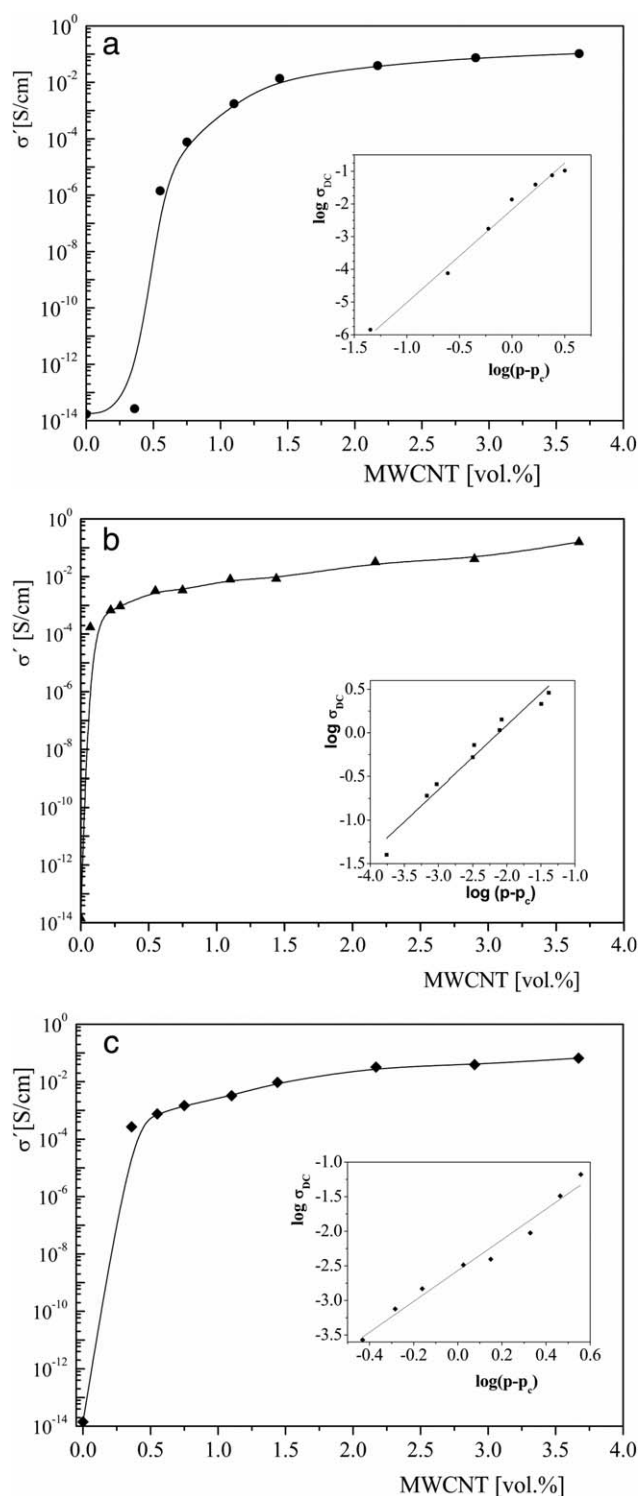


Figure 5. The $\sigma_{AC}(f)$ versus amount of MWCNT in vol % in composites prepared by melt mixing (a), and by solution casting in chloroform (b), and toluene (c). The inserts show plot of logarithm of σ_{DC} versus $\log(p-p_c)$ with (a) $t = 2.84 \pm 0.14$, $p_c \sim 0.49$ vol %, (b) $t = 1.33 \pm 0.14$, $p_c \sim 0.03$ vol %, and (c) $t = 1.75 \pm 0.22$, $p_c \sim 0.03$ vol %.

0.10 S/cm, and when measured by the 4-point DC method, the obtained value was 0.65 S/cm. The calculated percolation threshold for the PMMA/MWCNT composites prepared by

solution casting was 0.03 vol %. The values of the conductivity exponents t for the composites prepared by casting from toluene reached 1.75 ± 0.22 and for chloroform 1.33 ± 0.14 , respectively. The conductivity exponent t calculated for the solution cast samples was significantly lower than that calculated for the samples prepared by melt mixing (2.84 ± 0.14). Recently, Foygel *et al.*³⁰ studied conducting systems containing randomly dispersed fillers with different aspect ratios based on Monte Carlo simulations and found that the conductivity exponent substantially decreased with increasing filler aspect ratio. Indeed, for three dimensional (3D) systems comprising oblong objects, the t exponent is smaller than 2.0, and with decreasing MWCNT aspect ratios, higher t exponents (2.9 ± 0.3) have been calculated.³¹ In particular, for 3D systems of randomly oriented CNT, such as distributed CNT with aspect ratios in the range of 100 to 1000, the conductivity exponent has been shown to be 1.2–1.6, which is close to the conductivity exponent for 2D systems ($t = 1.1$ – 1.4).²⁶ For the composites prepared here by melt mixing, the higher values of the t exponent can be explained by the reductions in the lengths and aspect ratios of the MWCNT due to the high shear forces and local tensions resulting from mixing, as observed in SEM images. The lower conductivities of the melt mixed samples compared to the solution cast samples can also be explained by the destruction of the CNT during mixing. On the other hand, significantly higher t values have also been observed for semicrystalline systems, such as 3.3 for poly(vinyl chloride)/MWCNT,³² 3.8 for polycarbonate/MWCNT,³³ and 4.5 ± 0.2 for polypropylene/MWCNT, as reported by Logakis *et al.*³⁴ In all the aforementioned cases, the MWCNT aspect ratio corresponded to ~ 1000 . It was demonstrated that a crystalline layer formed around the CNT (*trans*-crystallinity) and prevented direct interactions between them, resulting in wide inter-particle distance distributions, leading to non-universal high t values.¹⁹ These significant changes in the crystallization behavior of the matrix upon the addition of CNT, resulted in increased crystallinity as well as in the appearance of a new crystallization peak (owing to *trans*-crystallinity) that was confirmed by differential scanning calorimetry.

Nanomechanical Properties

In the future, the prepared PMMA/CNT composites will be tested in gas sensor applications in our labs. Therefore a detailed investigation of their electrical properties was conducted. The mechanism of liquid or vapour sensing is based on the ability of polymer matrices to swell, where the local volumetric uptake will increase the conducting filler–filler distance and therefore the conductivity of the composite. For this reason, it is important to study the local surface mechanical properties of composite materials. Indentation tests were performed on the composite PMMA samples with CNT contents below and above the percolation threshold. The samples were prepared by melt mixing and solution casting from CHCl_3 . Tests were performed at several indentation depths, ranging from ~ 25 nm to 2000 nm, for all samples. The tests followed a trapezoidal load function, and the duration of each experiment was fixed at 15 s total time, that is, each segment (loading, hold, and unloading) lasted 5 s. Each experimental result presented here is the average of 5–6 tests with corresponding error bars. The

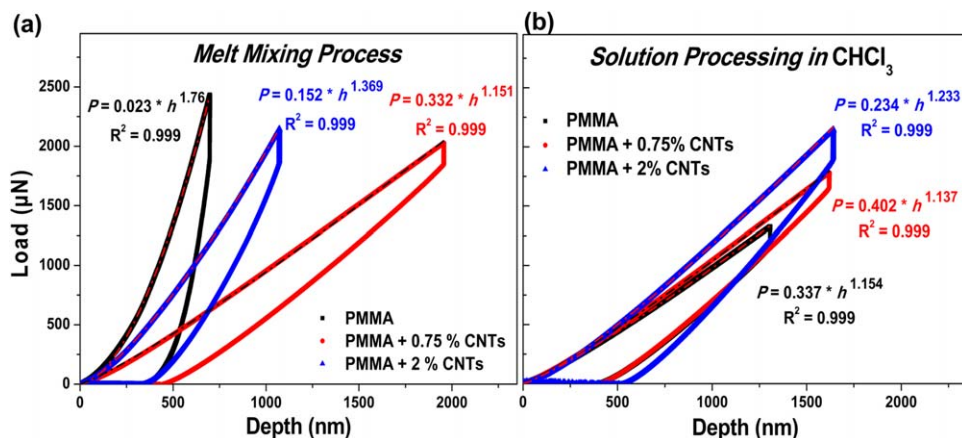


Figure 6. Load–unload curves of CNTs composite PMMA samples prepared by melt mixing (a), and solution processing in CHCl_3 (b). [Color figure can be viewed in the online issue, which is available at wileyonlinelibrary.com.]

distance between neighbouring indentation sites was more than $13 \mu\text{m}$ to avoid the lateral size of the plastic zone around the largest indents and exclude the mutual influence of individual indents.³⁵

Air indents were also performed following the same trapezoidal load function to investigate the tip adhesion onto the sample surface.^{36,37} Indentation tests were performed at various penetration depths reaching various maximum applied loads. The load–unload curves presented in Figure 6 reveal the elastoplastic behavior of the tested samples; it was observed that the samples prepared via the melt mixing process were more resistant to applied loads compared to the samples prepared by solution casting in CHCl_3 . In each graph, the fitting procedure of the loading curves, following a power law equation, is denoted. It can be observed that higher values of the exponential parameter were defined for PMMA and the PMMA/1.44 vol % CNT composite processed by melt mixing, indicating more resistant behavior and higher H and E_r values. The samples prepared via solution processing in CHCl_3 showed approximately the same tendency, with a low resistance to applied loads. However, the lowest resistance to applied loads was attributed to the neat PMMA matrix. The dispersion of CNT with CHCl_3 in the

PMMA matrix increased the resistance of the composite, indicating the improved mechanical performance of the PMMA matrix. However, as observed in Figure 6, during tip removal from the sample surface, there was a full recovery of the recorded displacement depth. This indicated that air indents should be performed to investigate the tip adhesion to the sample surface. In Figure 7, typical air indent curves are presented, and higher negative loads during tip retraction from the sample surface were recorded for the samples prepared with solution processing in CHCl_3 . As a result, it is expected that the H and E_r values obtained by the Oliver and Pharr model are affected by the tip–sample surface adhesion.³⁸

In Figure 8, the maximum applied load (P_{max}) values are plotted against the maximum displacement depth (h_{max}) for all tested samples. It is again noted that the melt mixing samples (neat PMMA matrix and composite containing 1.44 vol % CNT) presented higher resistances to the applied loads than did the solution processed samples. It is also evident that the addition of CNT to the PMMA matrix following solution casting in CHCl_3 slightly improved the resistance of the composite samples. Approximately the same behavior was observed for the PMMA/0.55 vol % CNT composite prepared by the melt

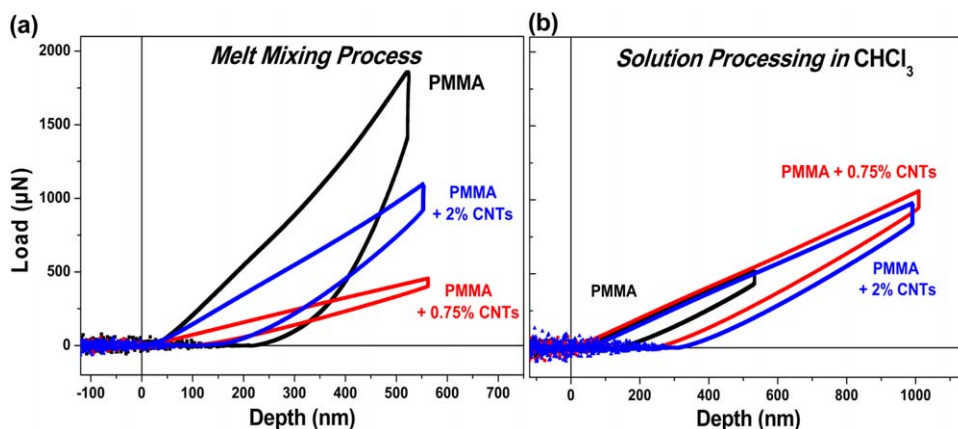


Figure 7. Air indents performed on the prepared composite samples and neat PMMA matrix indicating the adhesion of the sample's surface with the tip. [Color figure can be viewed in the online issue, which is available at wileyonlinelibrary.com.]

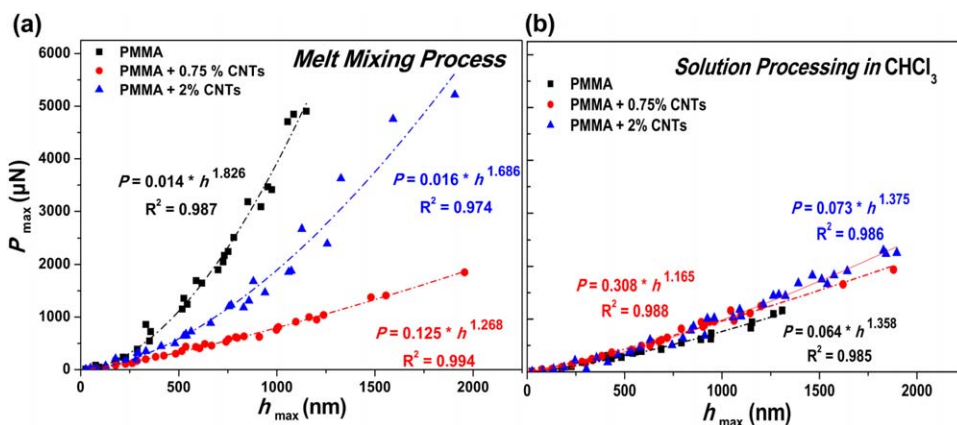


Figure 8. Maximum applied load (P_{max}) at the maximum displacement depth (h_{max}) for all composite samples and neat PMMA matrix. Power law fitting is also denoted for each curve. [Color figure can be viewed in the online issue, which is available at wileyonlinelibrary.com.]

mixing process. The H and E_r values are presented in Figure 9 as a function of h_{max} for all tested samples. Notably, the H and E_r values of the neat melt mixed PMMA matrix were higher (59% and 84%, respectively) than those measured for the neat solution cast in CHCl_3 PMMA matrix. Hence, the melt mixed PMMA matrix was stiffer than the solution cast PMMA. It can also be observed that the low addition of CNT in the composite samples prepared via melt mixing and solution casting in CHCl_3 did not improve the measured nanomechanical properties of the neat matrix. It was observed that the addition of 0.55 vol % CNT to the PMMA matrix via the melt mixing process reduced the H and E_r values by 65 and 88%, respectively;

whereas the addition of 1.44 vol % CNT resulted in 37 and 60% lower H and E_r values, respectively, compared with the neat matrix. On the other hand, solution processing in CHCl_3 resulted in almost the same H values for all samples (including the neat matrix and the 0.55 and 1.44 vol % CNT composite samples), and the composite samples 12% lower E_r values compared with the neat matrix.

The addition of CNT at levels below the percolation threshold for both processes resulted in approximately the same H and E_r values; but additions above the percolation threshold produced 42% and 70% higher H and E_r values, respectively, for the melt mixing process. Consequently, the dispersion of the MWCNT in

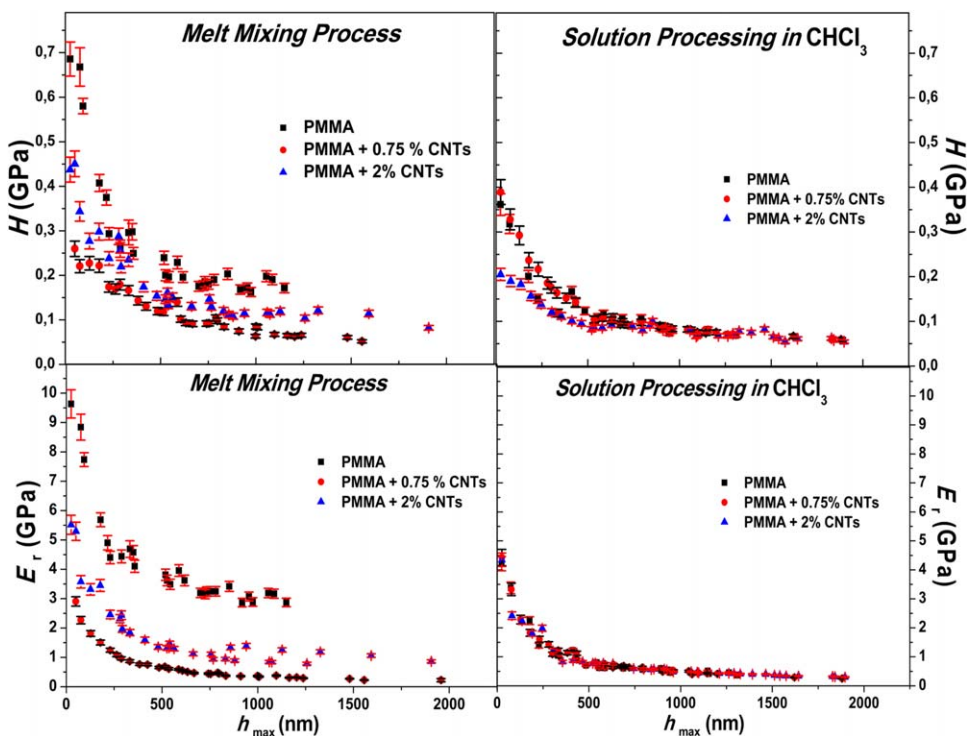


Figure 9. Hardness (H) and reduced modulus (E_r) values of the tested samples as a function of displacement depth (h_{max}). [Color figure can be viewed in the online issue, which is available at wileyonlinelibrary.com.]

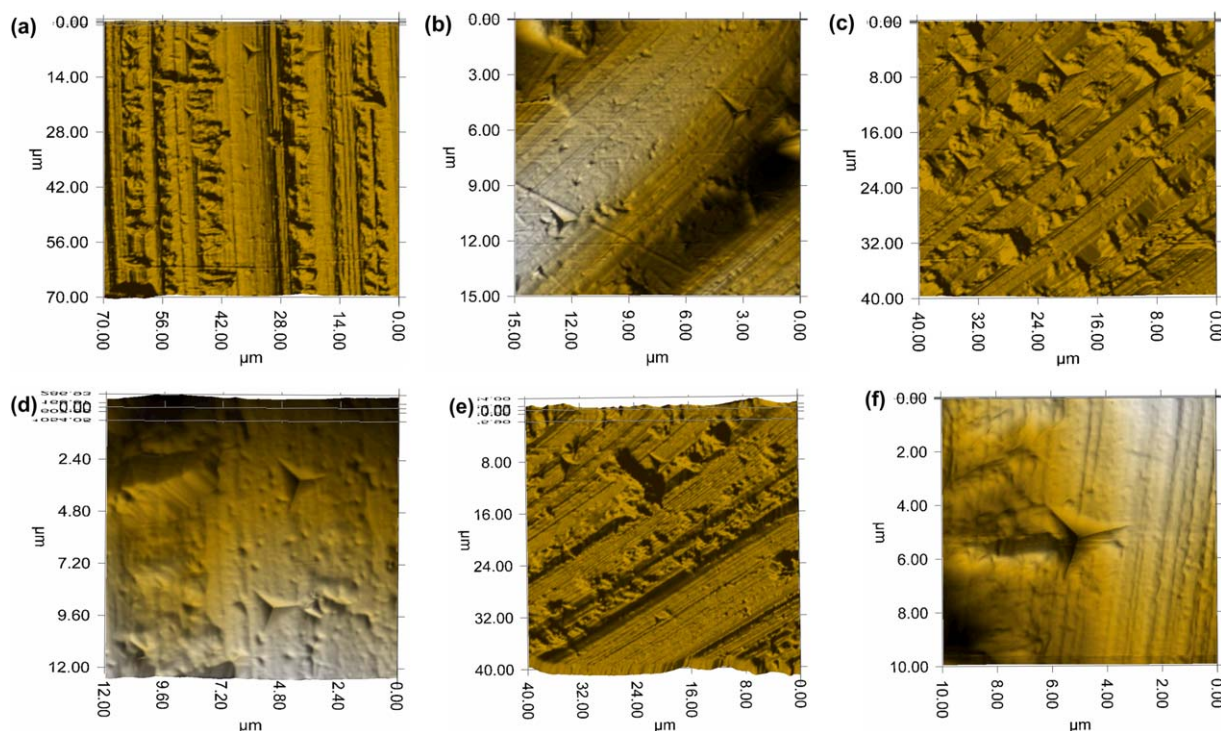


Figure 10. SPM images of (a) neat PMMA, (b) PMMA/0.55 vol % CNT, (c) PMMA/1.44 vol % CNT prepared by melt mixing; (d) neat PMMA, (e) PMMA/0.55 vol % CNT, and (f) PMMA/1.44 vol % prepared by solution casting from CHCl_3 . [Color figure can be viewed in the online issue, which is available at wileyonlinelibrary.com.]

the PMMA matrix was improved when the melt mixing process was used, resulting in better and more homogeneously distributed nanomechanical properties,^{39,40} as also observed by SEM study. The better dispersion of the CNT was attributed to the shortening of the CNT during melt mixing, which resulted in more homogenous nanomechanical properties. However, at the near surface, the H and E_r values were higher as a result of the surface roughness of the samples and the indentation size effect.⁴¹ Additionally, differences in H values were noted for the samples casted by solution processing in CHCl_3 compared to the expected behavior observed in Figures 6–8 due to the higher surface roughness of the samples and the small pile-ups around the indents (Figure 10). It should be noted that the formation of pile-ups around the indents indicates overestimation of the measured H and E_r values.⁴² In the literature, the measured H and E_r values of PMMA samples synthesized in tetrahydrofuran (THF)⁴³ and in CHCl_3 ⁴⁴ neat matrix are approximately the same as those estimated in this work. Olek *et al.*⁴⁴ reported that the addition of MWCNT to PMMA matrix with solution processing in CHCl_3 did not result in any improvements in the nanomechanical performance of the neat PMMA matrix. They claimed that the CNT displaced from their positions in the polymer matrix as a result of the flexibility and the small bending strength of the CNT.⁴⁵ Hence, during indentation testing of composite containing CNT, the tip primarily detects the mechanical properties of the polymer matrix. Consequently, good dispersion and increased concentrations of CNT within the PMMA matrix do not produce improvements in the mechanical efficiency of the composite material.⁴⁶ However,

composite materials with low additions of CNT and different polymeric matrices revealed improvements in their nanomechanical properties.⁴⁷ In summary, the PMMA/MWCNT composites prepared by melt mixing and/or solution casting presented adequate resistance to applied loads, with higher resistance observed for the melt mixed composites. However, the addition of CNT decreased the H and E_r values as a result of the poor dispersion or destruction of the CNT structure, with higher decreases in the H and E_r values observed for the melt mixed composites. Nevertheless, it was observed that the melt mixing process resulted in stiffer composites, rendering solution casted composites suitable materials for sensor applications because a soft or more elastic matrix is more suitable for swelling; therefore, these samples are suitable for testing as vapour sensors.

CONCLUSIONS

In this study, PMMA/MWCNT composites were prepared by melt mixing and solution casting in chloroform and in toluene. SEM study indicated that the PMMA/MWCNT composites prepared by both methods had good homogeneity, but the dispersion of the MWCNT in the PMMA matrix prepared by solution casting was better. Therefore, the PMMA/MWCNT composites prepared by solution casting displayed higher electrical conductivities and lower percolation thresholds than did those prepared by melt mixing. The highest value of σ' (f), 1.57×10^{-1} S/cm, was achieved in the samples prepared by solution casting in toluene at a loading of 3.67 vol % MWCNT; slightly lower

conductivities were achieved in the composites prepared from chloroform. The calculated percolation threshold was 0.03 vol % for the PMMA/MWCNT composites prepared by solution casting. A significantly higher percolation concentration of 0.49 vol % MWCNT was calculated for the samples prepared by melt mixing. The nanomechanical properties of the PMMA/MWCNT composites revealed sufficient resistance to applied loads for all prepared samples as well as elastoplastic behavior. The solution cast composites revealed softer behavior and higher adhesion to the tip surface. Furthermore, the addition of MWCNT to the PMMA matrix by both preparation methods resulted in decreased H and E_r values compared to the neat PMMA matrices. However, the solution cast PMMA/MWCNT composites displayed a lower reduction in H and E_r values, revealing the better dispersion of the CNT in the matrix structure. The adequate mechanical stability of the solution cast PMMA/MWCNT composites, in conjunction with their higher conductivity values, reveals the positive effect of solution processing on the properties of PMMA/MWCNT composites.

ACKNOWLEDGMENTS

The research was supported by project VEGA 2/0149/14 (Slovakia). Authors Skarmoutsou and Charitidis kindly acknowledge the financial support of the European Union (European Social Fund) and Greek national funds through the Operational Program "Education and Lifelong Learning" of the National Strategic Reference Framework (NSRF) - Research Funding Program: Heracleitus II. Investing in knowledge society through the European Social Fund. J. Prokeš thanks the Czech Grant Agency (13-00270S) for financial support.

REFERENCES

1. Iijima, S. *Nature* **1991**, *354*, 56.
2. Špitalský, Z.; Tasis, D.; Papagelis, K.; Galiotis, C. *J. Prog. Polym. Sci.* **2010**, *35*, 357.
3. McClory, C.; McNally, T.; Baxendale, M.; Pötschke, P.; Blau, W.; Ruether, M. *Eur. Polym. J.* **2010**, *46*, 854.
4. Broza, G.; Piszczek, K.; Schulte, K.; Sterzynski, T. *Compos. Sci. Technol.* **2007**, *6*, 890.
5. Mičušík, M.; Omastová, M.; Krupa, I.; Prokeš, J.; Pissis, P.; Logakis, E.; Pandis, Ch.; Pötschke, P.; Pionteck, J. *J. Appl. Polym. Sci.* **2009**, *113*, 2536.
6. Logakis, E.; Pandis, Ch.; Peoglos, V.; Pissis, P.; Pionteck, J.; Pötschke, P.; Mičušík, M.; Omastová, M. *Polymer* **2009**, *50*, 5103.
7. Gorga, R. E.; Cohen, R. E. *J. Polym. Sci. Part B – Polym. Chem.* **2004**, *42*, 2690.
8. Alig, I.; Pötschke, P.; Lellinger, D.; Skipa, T.; Pegel, S. *Polymer* **2012**, *53*, 24.
9. Du, F.; Fischer, J. E.; Wine, K. I. *J. Polym. Sci. Part B – Polym. Chem.* **2003**, *41*, 3333.
10. Kim, H. M.; Choi, M.-S.; Joo, J. *Phys. Rev. B.* **2006**, *74*, 054202.
11. Thostenson, E. T.; Ren, Z. F.; Choua, T.-W. *Compos. Sci. Technol.* **2001**, *61*, 1899.
12. Maa, P.-C.; Siddiquia, N. A.; Maromb, G.; Kim, J.-K. *Compos. Part A. Appl. Sci. Manuf.* **2010**, *41*, 1345.
13. Yuen, S.-M.; Ma, C.-C. M.; Chuang, C.-Y.; Yu, K.-C.; Wu, S.-H.; Yang, C.-C.; Wei, M.-H. *Compos. Sci. Technol.* **2008**, *68*, 963.
14. Omastová, M.; Pavlinec, J.; Pionteck, J.; Simon, F.; Košina, S. *Polymer* **1998**, *39*, 6559.
15. Park, S.; Vosguerichian, M.; Bao, Z. A. *Nanoscale.* **2013**, *5*, 1727.
16. Kumar, S.; Sharma, A.; Tripathi, B.; Srivastava, S.; Agrawal, S.; Singh, M.; Awasthi, K.; Vijay, Y. K. *Micron.* **2010**, *41*, 909.
17. Chen, H.; Muthuraman, H.; Stokes, P.; Zou, J.; Liu, X.; Wang, J.; Huo, Q.; Khondaker, S. I.; Zhai, L. *Nanotechnology* **2007**, *18*, 415606.
18. Bauhofer, W.; Kovacs, J. Z. *Compos. Sci. Technol.* **2009**, *69*, 1486.
19. Logakis, E.; Pandis, Ch.; Pissis, P.; Pionteck, J.; Pötschke, P. *Compos. Sci. Technol.* **2011**, *71*, 854.
20. Khatarri, Z.; Maghrabi, M.; McNally, T.; Jawad, S. A. *Physica B* **2012**, *407*, 759.
21. Slobodian, P.; Lengálová, A.; Sába, P.; Šlouf, M. *J. Reinforced. Plastics. Compos.* **2007**, *26*, 1705.
22. Material data sheet NC7000; Nanocyl, S. A. *Sambreville; Belgium*; 10 March **2009**.
23. King, R. B. *Int. J. Solids. Struct.* **1987**, *23*, 1657.
24. Oliver, W. C.; Pharr, G. M. *J. Mater. Res.* **1992**, *7*, 1564.
25. Sneddon, I. N. *Math. Proc. Cambridge Philos. Soc.* **1948**, *44*, 492.
26. Krause, B.; Boldt, R.; Pötschke, P. *Carbon.* **2011**, *49*, 1243.
27. Kremer, F.; Schönhal, A. *Broadband dielectric spectroscopy*; Springer-Verlag Berlin, **2003**.
28. von Jonscher, A. K. *Dielectric relaxation in solids. London; Chelsea Dielectrics*; **1983**.
29. Stauffer, D.; Aharony, A. *Introduction to percolation theory. Taylor and Francis. London*; **1998**.
30. Foygel, M.; Morris, R. D.; Anez, D.; French, S.; Sobolev, V. L. *Phys. Rev. B.* **2005**, *71*, 104201.
31. Logakis, E.; Pissis, P.; Pospiech, D.; Korwitz, A.; Krause, B.; Reuter, U.; Pötschke, P. *Eur. Polym. J.* **2010**, *46*, 928.
32. Mamunya, Y.; Boudenne, A.; Lebovka, N.; Ibos, L.; Candau, Y.; Lisunova, M. *Compos. Sci. Technol.* **2008**, *68*, 1981.
33. Pötschke, P.; Abdel-Goad, M.; Alig, I.; Dudkin, S. M.; Lellinger, D. *Polymer* **2004**; *45*; 8863.
34. Logakis, E.; Pollatos, E.; Pandis, Ch.; Peoglos, V.; Zuburtikudis, I.; Delides, C. G.; Vatalis, A.; Gjoka, M.; Syskakis, E.; Viras, E.; Pissis, P. *Compos. Sci. Technol.* **2010**; *70*; 328.
35. Rabkin, E.; Deuschle, J. K.; Baretzky, B. *Acta Mater.* **2010**, *58*, 1589.
36. Cao, Y.; Yang, D.; Soboyejoy, W. *J. Mater. Res.* **2005**, *20*, 2004.
37. Charitidis, C. A. *Ind. Eng. Chem. Res.* **2011**, *50*, 565.

38. Kohn, J. C.; Ebenstein, D. M. *J. Mech. Behav. Biomed. Mater.* **2013**, *20*, 316.
39. Haggemueller, R.; Gommans, H. H.; Rinzler, A. G.; Fischer, J. E.; Winey, I. *Chem. Phys. Lett.* **2000**, *330*, 219.
40. Jin, Z.; Pramoda, K. P.; Xu, G.; Goh, S. H. *Chem. Phys. Lett.* **2001**, *337*, 43.
41. Nix, W. D.; Gao, H. *J. Mech. Phys. Solids* **1998**, *46*, 411.
42. Lee, Y. H.; Hahn, J. H.; Nahm, S. H.; Jang, J. I.; Kwon, D. *J. Phys D; Appl. Phys.* **2008**, *41*, 074027.
43. Jee, A.-Y.; Lee, M. *Polym. Testing* **2010**, *29*, 95.
44. Olek, M.; Kempa, K.; Jurga, S.; Giersig, M. *NSTI-Nanotechnology Proceedings 2*. 2005, 167.
45. Wong, E. W.; Sheehan, P. E.; Lieber, C. M. *Science* **1997**, *277*, 1971.
46. Pavaor, P. V.; Gearing, B. P.; Gorga, R. E.; Bellare, A.; Cohen, R. E. *J. Appl. Polym. Sci.* **2004**, *92*, 439.
47. Charitidis, C. A.; Koumoulos, E. P.; Giorcelli, M.; Musso, S.; Jagadale, P.; Tagliaferro, A. *Polym. Compos.* **2013**, *34*, 1950.